

# Magnetic Resonance Fingerprinting with Total Nuclear Variation Regularisation

Imraj RD Singh<sup>1</sup>, Olivier Jaubert<sup>1</sup>, Bangti Jin<sup>1</sup>, Kris Thielemans<sup>2</sup>, and Simon Arridge<sup>1</sup>

<sup>1</sup>Department of Computer Science, University College London, Gower Street, London WC1E 6BT, UK

<sup>2</sup>Institute for Nuclear Medicine, University College London, London NW1 2BU, UK

## SYNOPSIS

Magnetic Resonance Fingerprinting (MRF) accelerates quantitative magnetic resonance imaging. The reconstruction can be separated into two problems: reconstruction of a set of multi-contrast images from k-space signals, and estimation of parametric maps from the set of multi-contrast images. In this study we focus on the former problem, while leveraging dictionary matching for the estimation of parametric maps. Two different sparsity promoting regularisation strategies were investigated: contrast-wise Total Variation (TV) which encourages image sparsity separately; and Total Nuclear Variation (TNV) which promotes a measure of joint edge sparsity. We found improved results using joint sparsity.

Keywords: Magnetic Resonance Fingerprinting, Synergistic Reconstruction, Low-Rankness

## SUMMARY OF FINDINGS

Low-rank direct inversion, TV and TNV regularised reconstruction of MRF data were tested on 2D BrainWeb phantoms. T1, T2 and proton density parametric maps were then obtained using dictionary matching. Parametric maps estimated with TNV had the lowest mean squared error.

## INTRODUCTION

Magnetic Resonance Fingerprinting (MRF) consists of taking a set of highly under-sampled measurements of multi-contrast images. Then, on a pixel-by-pixel basis, the multi-contrast images are dictionary matched to the underlying physical properties resulting in parametric maps. In this work we investigate sparsity based regularisation for multi-contrast image reconstruction, and the effect on dictionary matched parametric maps.

Sparsity based regularisation techniques such as Total Variation (TV)<sup>1</sup> can act to penalise edges, and therefore have a denoising effect on reconstructions. In addition to sparsity, it is observed that multi-contrast images of underlying tissue properties show significant joint structural features.<sup>2</sup> These features can be exploited through regularisation that promotes a measure of joint edge sparsity. Total Nuclear Variation (TNV) is a measure of joint edge sparsity that is known<sup>2-4</sup> to promote sparse, co-located and parallel edges. From observations of the MRF multi-contrast image set, it is hypothesised that through TNV regularisation the accuracy of parametric maps can be increased. Therefore we propose the novel use of TNV as a measure of joint edge sparsity for MRF reconstruction. This is distinct from previous work that exploits redundancy in the image contrasts,<sup>5</sup> as we exploit redundancy in the image gradients (edges).

## METHODS

The BrainWeb phantom ( $200 \times 200$  pixels)<sup>6,7</sup> was used as ground-truth parametric maps. On a pixel-by-pixel basis, the maps were converted to the ground truth multi-contrast image set using the Extended Phase Graph (EPG) formalism.<sup>8</sup> EPG simulates an ensemble of spins of particular tissue properties under the influence of a pulse sequence. The pulse sequence was defined as linear ramps of flip angles with constant repetition time.<sup>9</sup> Between each flip angle a read-out is taken as a single radial spoke that is rotated

by the golden angle between read-outs. The MRF signal is obtained by taking under-sampled k-space measurements with a non-uniform Fast Fourier Transform (nuFFT)<sup>10</sup> of the ground truth multi-contrast image set. Additive complex white Gaussian noise was added to the k-space signal to reduce the overall peak signal-to-noise to 40 dB.

The dictionary was simulated using EPG for a range of realistic T1 [100:10:4000 ms] and T2 [20:2:600 ms] values, whilst ensuring that T1 > T2 for all dictionary entries. The dimensionality of the multi-contrast image reconstruction was drastically reduced through projecting the solution into a low-rank subspace of the dictionary.<sup>11,12</sup> The low-rank subspace was determined by taking a singular value decomposition and using the first ten right singular vectors corresponding to the ten largest singular values. Each pixel is projected into this low-rank subspace resulting in ten multi-contrast singular images.

TV and TNV sparsity based regularisation techniques were implemented. TNV extends TV<sup>1,3,4</sup> by enforcing low-rankness in the pixel-wise Jacobian of image gradients along the set of images.

The optimisation problem was cast:<sup>3</sup>

$$\min_{\mathbf{X}} \delta_{\epsilon}(\mathbf{A}\mathbf{X} - \mathbf{S}) + \mathcal{R}(\nabla\mathbf{X})$$

The TV/TNV regularisation is denoted as  $\mathcal{R}$  and the indicator function  $\delta_{\epsilon}(\mathbf{A}\mathbf{X} - \mathbf{S})$  is defined as:

$$\delta_{\epsilon}(\mathbf{A}\mathbf{X} - \mathbf{S}) = \begin{cases} 0 & \|\mathbf{A}\mathbf{X} - \mathbf{S}\|_2 \leq \epsilon, \\ \infty & \|\mathbf{A}\mathbf{X} - \mathbf{S}\|_2 > \epsilon \end{cases}$$

where  $\mathbf{A}$  is a block operator composed of forward models that combine linear operators for under-sampling, low-rank subspace projection and Fourier transform.  $\mathbf{S}$  is the MRF signal and  $\mathbf{X}$  is the set of singular images to be reconstructed. The tolerance  $\epsilon$  is used as a regularisation parameter, whereby error can be allowed into the data fitting term and the regularisation term  $\mathcal{R}(\nabla\mathbf{X})$  is penalised more.<sup>3</sup> The notation  $\nabla$  denotes taking the image gradient. The Primal-Dual Hybrid Gradient (PDHG) algorithm<sup>13</sup> was used to reconstruct in both the TV and TNV cases in order to deal with the non-smoothness of these regularisation functionals. Direct inversion was obtained through a density compensated adjoint nuFFT.

The cosine similarity metric was used to match individual pixel-wise evolutions of the singular images to a compressed dictionary entry, with the T1 and T2 values of that entry mapped back to the pixel. Proton density (PD) was determined from the scale of the pixel evolution.

## RESULTS

Solutions with TV and TNV regularisation were obtained with a range of  $\epsilon$  values. Figure 2 gives the effect of the  $\epsilon$  values on the Mean Squared Error (MSE) of dictionary matched parametric maps. The data-fitting term  $\|\mathbf{S} - \mathbf{A}\mathbf{X}\|_2$  is used to give an indication of the (inverse of) regularisation strength. The first five singular images are given in Figure 3 for direct inversion, TV and TNV solutions. The best TV solution is shown with  $\epsilon = \sqrt{30}$  and best TNV solution with  $\epsilon = \sqrt{35}$ . Furthermore, the resulting parametric maps are given in Figure 4.

## DISCUSSION AND CONCLUSION

Direct inversion resulted in MSE an order of magnitude larger than regularised reconstruction with TV or TNV. Out of the two regularisation methods TNV provided less error regardless of  $\epsilon$  value for T2 and PD maps. This can be seen in Figure 2 where the TNV curves lie below TV. For T1 maps there are improvements in MSE for TNV with  $\|\mathbf{S} - \mathbf{A}\mathbf{X}\|_2 < 6.15$ . Through leveraging the low-rank subspace of the dictionary, the majority of statistical information from the singular images is concentrated in the first singular images. From figure 3, TNV reduces MSE on the first, third and fourth singular images as compared with TV. This results TNV outperforming TV on parametric maps. With reductions in MSE of 2.4%, 32.6% and 23.6% for whole brain T1, T2 and PD maps.

The synergistic action of TNV, which penalises rank two pixel-wise Jacobians such that they are rank one, aligns the edge set along the set of singular images. This results in appreciable reduction in MSE on parametric maps as compared with TV. Sparsity based synergistic regularisation presents a method to increase accuracy of reconstructed parametric maps for MRF. Code and data available here.

## **ACKNOWLEDGMENTS**

This work was supported by EPSRC Centre for Doctoral Training in Intelligent, Integrated Imaging In Healthcare (EP/S021930/1). Freely available software from<sup>8,10,14,15</sup> was utilised in this research.

## REFERENCES

- <sup>1</sup> Leonid I. Rudin, Stanley Osher, and Emad Fatemi. Nonlinear total variation based noise removal algorithms. *Physica D: Nonlinear Phenomena*, 60(1-4):259–268, November 1992.
- <sup>2</sup> Simon R. Arridge, Matthias J. Ehrhardt, and Kris Thielemans. (an overview of) synergistic reconstruction for multimodality/multichannel imaging methods. *Philosophical Transactions of the Royal Society A: Mathematical, Physical and Engineering Sciences*, 379(2200):20200205, May 2021.
- <sup>3</sup> David S Rigie and Patrick J La Rivière. Joint reconstruction of multi-channel, spectral CT data via constrained total nuclear variation minimization. *Physics in Medicine and Biology*, 60(5):1741–1762, feb 2015.
- <sup>4</sup> Joan Duran, Michael Möller, Catalina Sbert, and Daniel Cremers. Collaborative total variation: A general framework for vectorial TV models. *CoRR*, abs/1508.01308, 2015.
- <sup>5</sup> Aurélien Bustin, Gastão Lima da Cruz, Olivier Jaubert, Karina Lopez, René M. Botnar, and Claudia Prieto. High-dimensionality undersampled patch-based reconstruction (HD-PROST) for accelerated multi-contrast MRI. 81(6):3705–3719, March 2019.
- <sup>6</sup> B. Aubert-Broche, A.C. Evans, and D.L. Collins. A new improved version of the realistic digital brain phantom. *NeuroImage*, 32(1):138–145, 2006.
- <sup>7</sup> B. Aubert-Broche, M. Griffin, G.B. Pike, A.C. Evans, and D.L. Collins. Twenty new digital brain phantoms for creation of validation image data bases. *IEEE Transactions on Medical Imaging*, 25(11):1410–1416, 2006.
- <sup>8</sup> Matthias Weigel. Extended phase graphs: Dephasing, RF pulses, and echoes - pure and simple. *Journal of Magnetic Resonance Imaging*, 41(2):266–295, April 2014.
- <sup>9</sup> Pedro A. Gómez, Matteo Cencini, Mohammad Golbabaee, Rolf F. Schulte, Carolin Pirkl, Izabela Horvath, Giada Fallo, Luca Peretti, Michela Tosetti, Bjoern H. Menze, and Guido Buonincontri. Rapid three-dimensional multiparametric MRI with quantitative transient-state imaging. *Scientific Reports*, 10(1), August 2020.
- <sup>10</sup> J.A. Fessler and B.P. Sutton. Nonuniform fast fourier transforms using min-max interpolation. *IEEE Transactions on Signal Processing*, 51(2):560–574, 2003.
- <sup>11</sup> Debra F. McGivney, Eric Pierre, Dan Ma, Yun Jiang, Haris Saybasili, Vikas Gulani, and Mark A. Griswold. Svd compression for magnetic resonance fingerprinting in the time domain. *IEEE Transactions on Medical Imaging*, 33(12):2311–2322, 2014.
- <sup>12</sup> Jakob Assländer, Martijn A. Cloos, Florian Knoll, Daniel K. Sodickson, Jürgen Hennig, and Riccardo Lattanzi. Low rank alternating direction method of multipliers reconstruction for MR fingerprinting. *Magnetic Resonance in Medicine*, 79(1):83–96, March 2017.
- <sup>13</sup> Antonin Chambolle and Thomas Pock. A first-order primal-dual algorithm for convex problems with applications to imaging. *Journal of Mathematical Imaging and Vision*, 40(1):120–145, December 2010.
- <sup>14</sup> Mohammad Golbabaee, Guido Buonincontri, Carolin Pirkl, Marion Menzel, Bjoern Menze, Mike Davies, and Pedro Gomez. Compressive mri quantification using convex spatiotemporal priors and deep auto-encoders, 2020.
- <sup>15</sup> Gal Mazor, Lior Weizman, Assaf Tal, and Yonina C. Eldar. Low rank magnetic resonance fingerprinting. In *2016 38th Annual International Conference of the IEEE Engineering in Medicine and Biology Society (EMBC)*, pages 439–442, 2016.

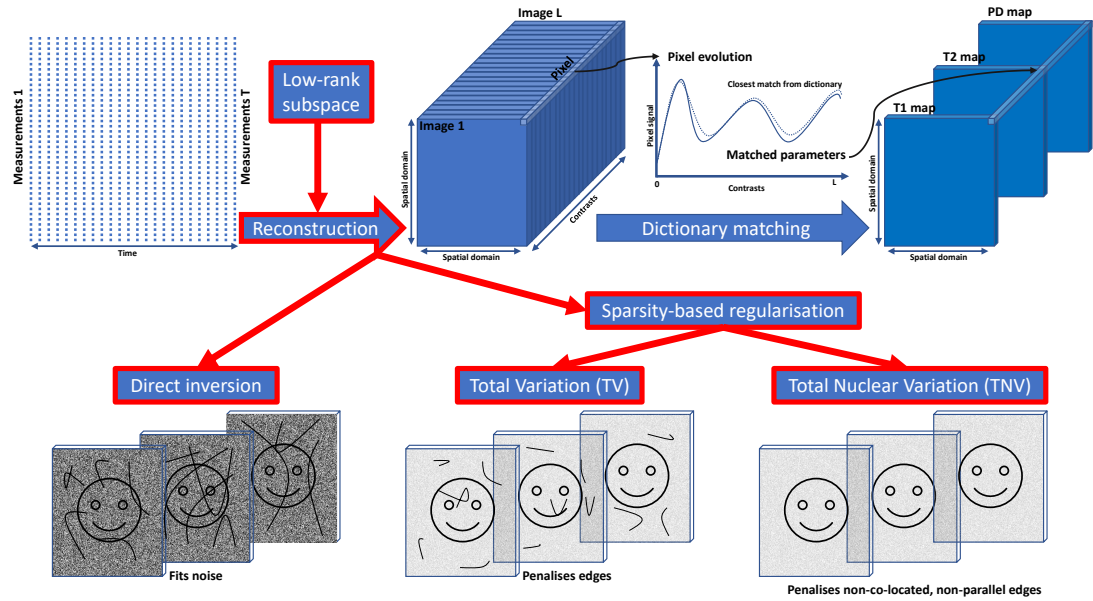


**Figure 1.** Illustrative diagram of the framework developed. The linear inverse problem of multi-contrast reconstruction was investigated with sparsity based regularisation techniques. Total variation promotes edge sparsity, whereas total nuclear variation promotes joint edge sparsity.

**Table 1.** Results on white and gray matter with best performing TV and TNV regularisation,  $\epsilon = \sqrt{30}$  and  $\epsilon = \sqrt{35}$  respectively.

White/Gray Matter	Parametric Map	Direct Inversion	Total Variation	Total Nuclear Variation
WM	T1 (s)	0.051	0.0046	0.0057
	T2 (s)	0.00075	5.3e-5	4.3e-5
	PD	0.054	0.0022	0.0021
GM	T1 (s)	0.072	0.013	0.0096
	T2 (s)	0.0027	0.00030	0.00022
	PD	0.060	0.0055	0.0034

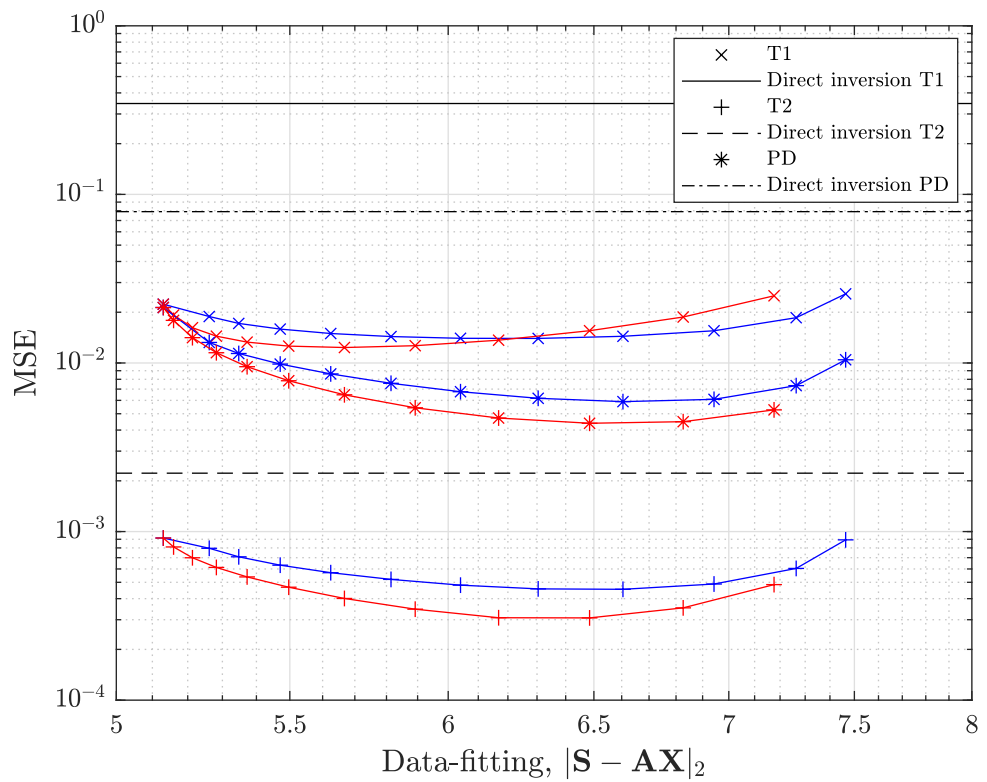


**Figure 2.** The colours correspond to **total variation** and **total nuclear variation**. The lowest error for TV and TNV was with  $\varepsilon = \sqrt{30}$  and  $\varepsilon = \sqrt{35}$  respectively. The data-fitting value gives an indication of the (inverse of) the regularisation strength. The MSE is the mean squared error of the corresponding parametric maps over the whole brain.

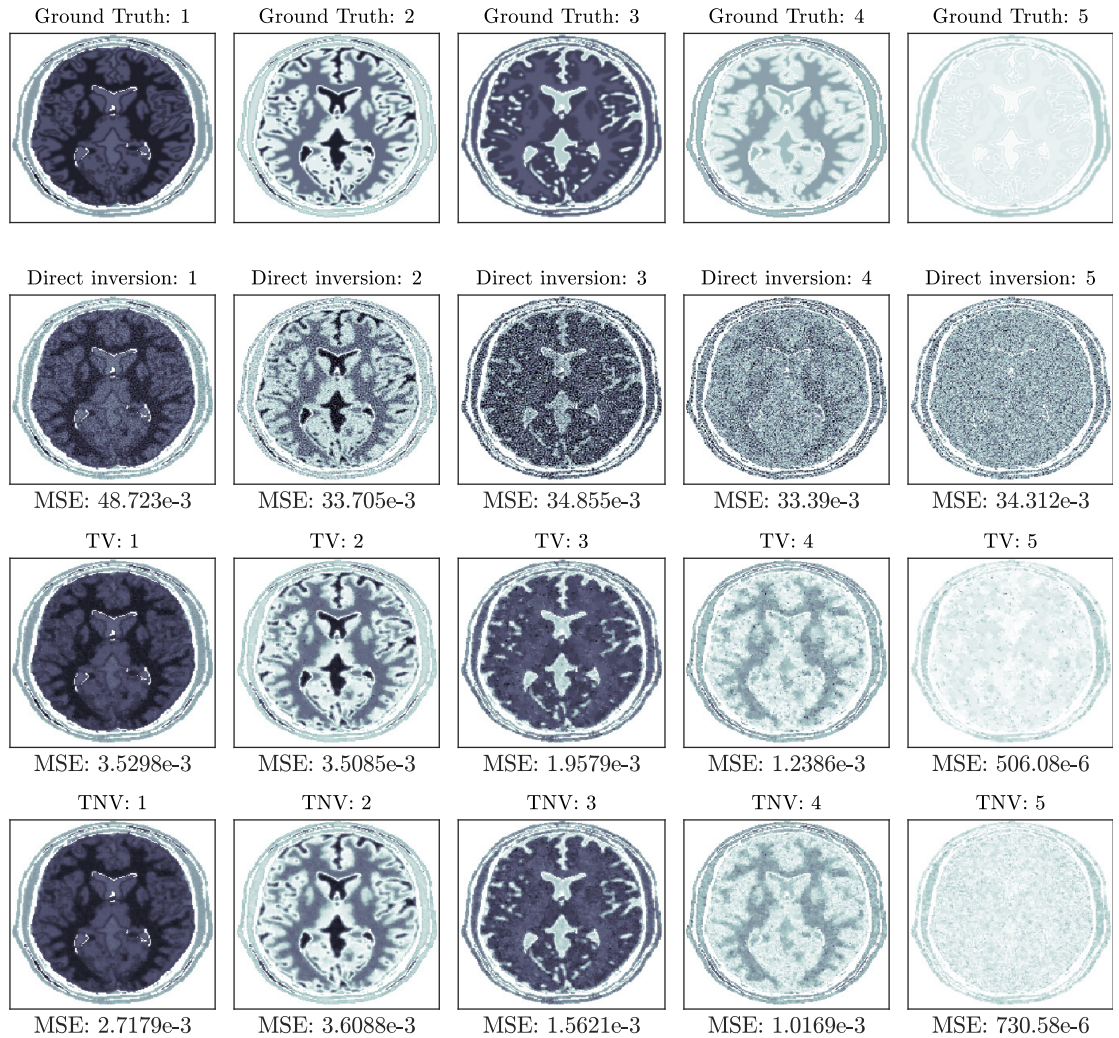


**Figure 3.** First five ground truth singular images, and images reconstructed with direct inversion, total variation ( $\epsilon = \sqrt{30}$ ) and total nuclear variation ( $\epsilon = \sqrt{35}$ ). Mean squared error (MSE) on all the reconstructed singular images. The colour bar limits were kept consistent between the same singular images.

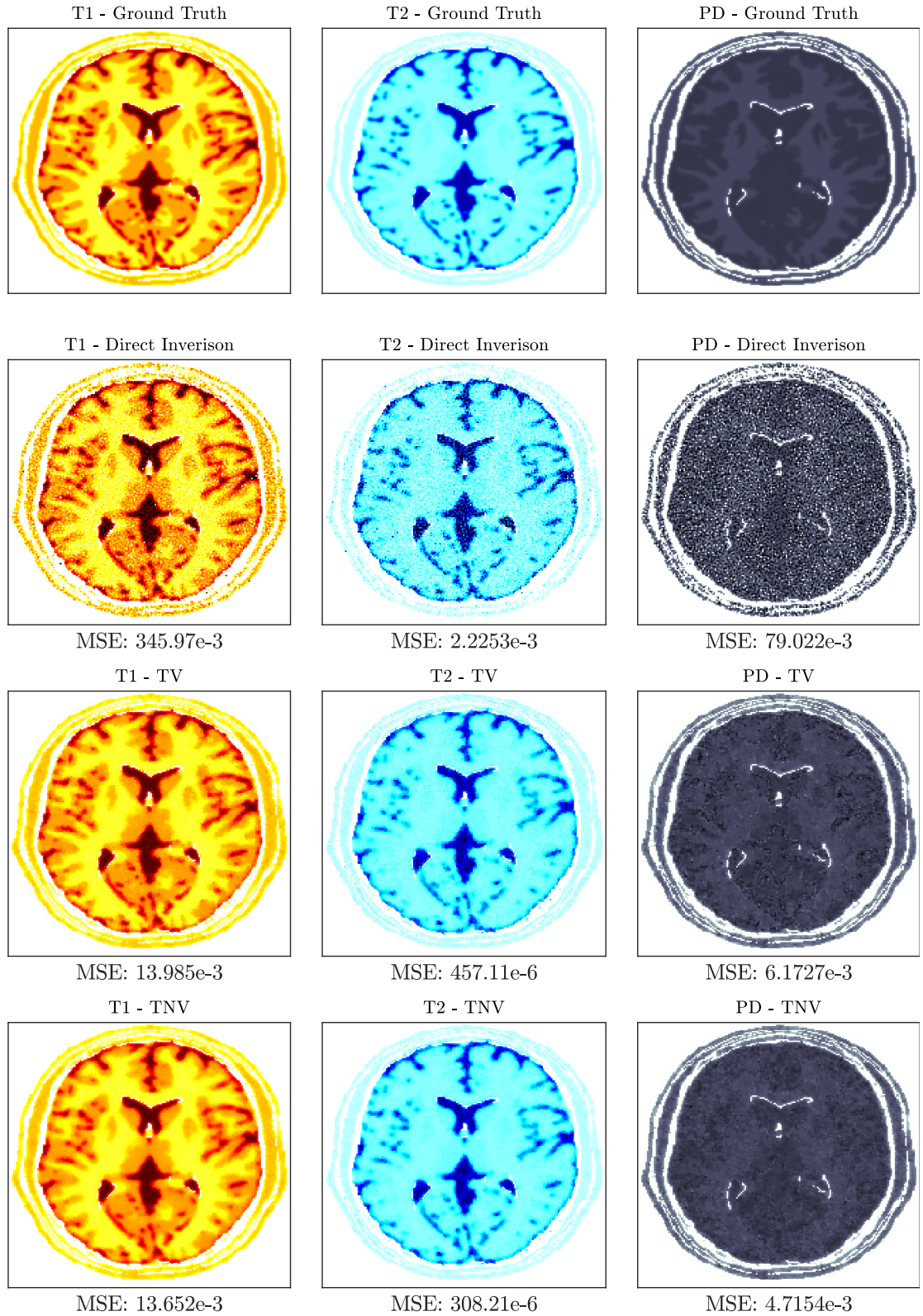


**Figure 4.** Comparison between dictionary matched total variation (TV) and total nuclear variation (TNV) solutions. Mean squared error (MSE) on T1, T2 and PD parametric maps. The colour bar limits were kept consistent between the same parametric maps.